REPORT DOCUMENTATION PAGE

Form Approved OMB NO. 0704-0188

1. REPORT DATE (DD-MM-YYYY)	2. REPORT TYPE	3. DATES COVERED (From - To)
09-09-2008	Final Report	1-Oct-2007 - 30-Jun-2008

4. TITLE AND SUBTITLE

Non-equilibrium phonon processes and degradation in gigahertz nanoscale mechanical resonators

5a. CONTRACT NUMBER
W911NF-07-1-0640

5b. GRANT NUMBER

5c. PROGRAM ELEMENT NUMBER
611102

6. AUTHORS

Gerald J. Iafrate, Andrey A. Kiselev

5d. PROJECT NUMBER

5e. TASK NUMBER

5f. WORK UNIT NUMBER

7. PERFORMING ORGANIZATION NAMES AND ADDRESSES

North Carolina State University
Office of Contract and Grants
Leazar Hall Lower Level- MC
Raleigh, NC 27695 -7214

8. PERFORMING ORGANIZATION REPORT NUMBER

9. SPONSORING/MONITORING AGENCY NAME(S) AND ADDRESS(ES)

U.S. Army Research Office
P.O. Box 12211
Research Triangle Park, NC 27709-2211

10. SPONSOR/MONITOR'S ACRONYM(S)
ARO

11. SPONSOR/MONITOR'S REPORT NUMBER(S)
53350-EG-II.1

12. DISTRIBUTION AVAILIBILITY STATEMENT

Approved for Public Release; Distribution Unlimited

13. SUPPLEMENTARY NOTES

The views, opinions and/or findings contained in this report are those of the author(s) and should not contrued as an official Department of the Army position, policy or decision, unless so designated by other documentation.

14. ABSTRACT

Nonequilibrium phonon processes and related degradation effects were treated for a Euler-Bernoulli flexural beam undergoing scaling from the micro to the nano spatial regime. For the scaling lengths under consideration, the lowest resonator mode is in the frequency range of 1-10 GHz. In a Euler-Bernoulli-Boltzmann framework, an analysis of the internal phonon dynamics and flow in the flexural beam is conducted, and dissipative losses are evaluated. in limiting cases, two major intrinsic dissipative mechamisms are operative, one dur to the diffusive spatial redistribution of phonons resulting in heat transfer and thermoelastic loss, and the other due to the thermalization of the local phonon population distorted by strain

15. SUBJECT TERMS

NEMS losses, dissipative resonator dynamics, gigahertz resonators

16. SECURITY CLASSIFICATION OF:			17. LIMITATION OF ABSTRACT	15. NUMBER OF PAGES	19a. NAME OF RESPONSIBLE PERSON
a. REPORT	b. ABSTRACT	c. THIS PAGE			Gerald Iafrate
U	U	U	SAR		19b. TELEPHONE NUMBER 919-513-2310

Report Title

Non-equilibrium phonon processes and degradation in gigahertz nanoscale mechanical resonators

ABSTRACT

Nonequilibrium phonon processes and related degradation effects were treated for a Euler-Bernoulli flexural beam undergoing scaling from the micro to the nano spatial regime. For the scaling lengths under consideration, the lowest resonator mode is in the frequency range of 1-10 GHz. In a Euler-Bernoulli-Boltzmann framework, an analysis of the internal phonon dynamics and flow in the flexural beam is conducted, and dissipative losses are evaluated. in limiting cases, two major intrinsic dissipative mechamisms are operative, one dur to the diffusive spatial redistribution of phonons resulting in heat transfer and thermoelastic loss, and the other due to the thermalization of the local phonon population distorted by strain resulting in a manifestation of the Akhiezer effect. In the frequency domain of interest,these two loss mechanisms loss their distinctive character with decreased scaling and transition to a unified dissipative process.

List of papers submitted or published that acknowledge ARO support during this reporting period. List the papers, including journal references, in the following categories:

(a) Papers published in peer-reviewed journals (N/A for none)

"Phonon dynamics and phonon assisted losses in Euler-Bernoulli nanobeams", A.A.Kiselev, G.J.Iafrate, North Carolina State University, Phys.RevB. 77, 205436 (2008)

Number of Papers published in peer-reviewed journals: 1.00

(b) Papers published in non-peer-reviewed journals or in conference proceedings (N/A for none)

Number of Papers published in non peer-reviewed journals: 0.00

(c) Presentations

Number of Presentations: 0.00

Non Peer-Reviewed Conference Proceeding publications (other than abstracts):

Number of Non Peer-Reviewed Conference Proceeding publications (other than abstracts): 0

Peer-Reviewed Conference Proceeding publications (other than abstracts):

Number of Peer-Reviewed Conference Proceeding publications (other than abstracts): 0

(d) Manuscripts

Number of Manuscripts: 0.00

Number of Inventions:

Graduate Students

NAME	PERCENT_SUPPORTED
FTE Equivalent:	
Total Number:	

Names of Post Doctorates

NAME	PERCENT_SUPPORTED
FTE Equivalent:	
Total Number:	

Names of Faculty Supported

NAME	PERCENT_SUPPORTED	National Academy Member
Andrey A. Kiselev	0.25	No
Gerald J. Iafrate	0.50	No
FTE Equivalent:	**0.75**	
Total Number:	**2**	

Names of Under Graduate students supported

NAME	PERCENT_SUPPORTED
FTE Equivalent:	
Total Number:	

Student Metrics

This section only applies to graduating undergraduates supported by this agreement in this reporting period

The number of undergraduates funded by this agreement who graduated during this period:	0.00
The number of undergraduates funded by this agreement who graduated during this period with a degree in science, mathematics, engineering, or technology fields:	0.00
The number of undergraduates funded by your agreement who graduated during this period and will continue to pursue a graduate or Ph.D. degree in science, mathematics, engineering, or technology fields:	0.00
Number of graduating undergraduates who achieved a 3.5 GPA to 4.0 (4.0 max scale):	0.00
Number of graduating undergraduates funded by a DoD funded Center of Excellence grant for Education, Research and Engineering:	0.00
The number of undergraduates funded by your agreement who graduated during this period and intend to work for the Department of Defense	0.00
The number of undergraduates funded by your agreement who graduated during this period and will receive scholarships or fellowships for further studies in science, mathematics, engineering or technology fields:	0.00

Names of Personnel receiving masters degrees

NAME
Total Number:

Names of personnel receiving PHDs

NAME
Total Number:

Names of other research staff

NAME	PERCENT_SUPPORTED
FTE Equivalent:	
Total Number:	

Sub Contractors (DD882)

Inventions (DD882)

Non-Equilibrium Phonon Processes and Degradation
in Gigahertz Nanoscale Mechanical Resonators

G. J. Iafrate (PI)
gjiafrate@ncsu.edu
North Carolina State University, Raleigh, NC 27695

Report Summary

Objective:

The objective of this study is to identify and quantify the loss and degradation mechanisms relevant to frequency control resonator performance as the resonator dimensions reduce to the nanodimensional spatial scale. The Department of the Army interest in scaling such devices into the nanodimensional region arises from the technical notion that such resonators can be designed to operate at frequencies into the low GHz region thus providing a low cost, integratable NEMS solid state device option for ultrafast frequency control electronic applications relevant to jam resistant secure communications. Inherent in the nanoscale domain is the dynamics of non-equilibrium phonon processes which play a central role in orchestrating loss mechanisms in general and in trade off of surface to volume effects as the resonator scales down. In this study, use is made of the Euler-Bernoulli-Boltzmann approach to capture and study the essence of the dominant physical considerations.

Approach:

The technical approach considers non-equilibrium heat generation and redistribution processes from mechanical strain during high frequency NEMS operation beyond the conventional heat diffusion and local temperature approximation. A semiclassical phonon dynamical picture is introduced to go beyond the conventional models. Scaling laws relevant to the appropriate phonon transport regimes and their transition boundaries are delineated, analyzed, and compared with results of detailed microscopic descriptions. Thus, the research approach involves scaling analysis, coupled with analytical and numerical modeling of phonon flow and heat redistribution in nanoscale resonators. Specifically, the following technical milestones were pursued:

1. Establish a picture of the beam dynamics in a non-equilibrium thermodynamical

framework. This requires a more refined look at the approximations of the Euler-Bernoulli equation with shear corrections to the beam dynamics, and generalizations of stress-strain relations in the presence of thermal gradients.

2. For intrinsic phonon-mediated dissipation mechanisms, formulate scaling laws based on relations between the key spatial and temporal characteristics of phonons, i.e., mean free path l_{ph} and phonon relaxation time τ_{ph}, and the relevant physical parameters of the NEMS structure, that is beam thickness t, length L, and resonator operational frequency ν.

3. Scaling laws relevant to the appropriate phonon transport regimes and their transition boundaries will be analyzed and compared with results of more microscopic analysis and theory.

4. Formulate robust treatment of phonons under non-equilibrium thermodynamic conditions in flexural nanobeams by introducing Boltzmann framework for description of phonon transport; conduct analysis of internal thermal phonon flow inside the beam.

5. Develop a reliable quantification of the Q factor in presence of non-diffusive phonon transport.

Accomplishments:

- Material parameters were successfully identified for the basic high frequency NEMS resonator designs; "operational frequency vs. spatial dimensions" maps have been established for the NEMS resonator from the Euler-Bernoulli equation.
- Major intrinsic dissipative mechanisms related to thermoelastic loss and phonon-phonon interactions and their scaling properties have been identified and strategically mapped to provide insightful physical analysis.
- From the developed scaling studies, it is theoretically noted that, in the 1–10 GHz operational frequency regime, the NEMS resonator thermal dynamics routinely goes beyond the limits of the local temperature approximation, not at all due to the often considered time constraint of the high frequency limit (which requires $\nu \approx \tau_{ph}^{-1}$, with $\tau_{ph} \approx 10$ps at room temperature), but, in contrast, due to sharp spatial inhomogeneity in strain pattern induced by flexure across the thin ($t < l_{ph}$, with $l_{ph} \approx 50$nm at T=300 K in

Si) beam cross section. This spatial consideration leads to rapid ballistic transfer of phonons across the beam and suppression of the dissipation mechanism associated with the entropy production due to inter-branch phonon-phonon thermal equilibration. The theoretical analysis is formulated and conducted in the Boltzmann framework to capture the proper phonon dynamics.

Journal Publication:

Results of extensive analysis and conclusions were recently published by A. A. Kiselev and G. J. Iafrate in Phy. Rev. B. 77, 205436 (2008); Publication is attached as Appendix A; detail summary, conclusion, and bibliography is contained therein.

Appendix A:

Phonon dynamics and phonon assisted losses in Euler-Bernoulli nanobeams

A. A. Kiselev*
HRL Laboratories LLC, Malibu, California 90265, USA

G. J. Iafrate
Department of Electrical and Computer Engineering, North Carolina State University, Raleigh, North Carolina 27695, USA
(Received 26 February 2008; published 30 May 2008)

Nonequilibrium phonon processes and related degradation effects are treated for a Euler-Bernoulli flexural beam undergoing scaling from a micro to nanospatial regime. For the scaling lengths under consideration, the lowest resonator mode is in the frequency range of 1–10 GHz. In this range, it is found that the beam thermal environment routinely exceeds the limits of validity for the local temperature approximation; this is due to sharp inhomogeneities in strain pattern across the thin beam cross sections induced by flexural motion as opposed to the often assumed temporal dynamics of high frequency operation. In a Euler-Bernoulli-Boltzmann framework, an analysis of the internal phonon flow in the flexural beam is conducted, and dissipative losses are evaluated. The complexity of the microscopic phonon dynamics is delineated and strategically graphed in terms of the parameters characterizing the flexural beam and the phonon system therein. In limiting cases, two major intrinsic dissipative mechanisms are operative, one due to the diffusive spatial redistribution of phonons resulting in heat transfer and thermoelastic loss, and the other due to thermalization of the local phonon population distorted by strain resulting in the manifestation of the Akhiezer effect. In the frequency domain of interest, these two loss mechanisms lose their distinctive character with decreased spatial scaling and transition to a unified dissipative process governed by the ballistic phonon transfer across the beam.

DOI: 10.1103/PhysRevB.77.205436 PACS number(s): 66.70.−f, 63.22.Gh, 62.80.+f

I. INTRODUCTION

Nanoelectromechanical systems (NEMS) have emerged as a very attractive concept for miniaturized devices, resonators, and actuators in application areas spanning the broad fields of metrology, engineering, life science, and medicine.[1,2] In particular, microsized resonators and cantilevers have been workhorse devices for light-weight, on-chip, and high-quality (high-Q) elements for frequency control electronics as well as actuator and sensor components for smart systems. As such devices are scaled from the micro to the nanolength scale, the lowest resonator mode of operation increases into a desirable high frequency range of 1–10 GHz. In this frequency range, the key question of concern becomes whether there are fundamental intrinsic physical limitations that come into play that might prohibit high-Q operation; this question provides the main motivation for our work.

Numerous mechanisms have been proposed previously as possible limitations to the quality factors of micro and nanoresonators.[3–6] Some mechanisms can be identified as *extrinsic* to the microresonator and, thus, in principle, can be suppressed by engineering design. For example, air damping can be eliminated in the vacuum-operated resonators. As well, doping impurities, the effect of the attachment and/or support structure, and surface absorption-desorption processes can also be considered as external mechanisms. *Intrinsic* loss mechanisms, on the other hand, persist due to the inherent material properties of the beam. For example, intrinsic phonon-mediated dissipation mechanisms are related to the processes of heat redistribution and entropy production. This happens during beam mechanical dynamics because spatially inhomogeneous strain is induced in the beam material by the motional flexure. Local compression and dilation directly affects the phonon dispersion, thereby leading to the creation of nonequilibrium phonon distributions, temperature gradients, and, consequently, heat transfer.

In lowest order, these processes are most simply treated by the standard theory of thermoelasticity that essentially relies on the validity of the classical heat diffusion law, the so-called Fourier's law,[5,7,8] where heat flow is proportional to the macroscopic temperature gradient in the material and the thermal conductivity is the coefficient of proportionality. This lowest order thermoelastic methodology does not include temporal relaxation or higher order non-Fourier heat flow effects. In this regard, Cattaneo and Vernotte introduced a heuristic temporal relaxation time into the Fourier heat flow process to generate a hyperbolic heat equation, which describes a nondiffusive heat transfer by means of the quickly decaying heat waves. In particular, with respect to the losses in NEMS, Sun *et al.*[9] built on the temporal relaxation approach by incorporating a non-Fourier heat flow term into their analysis; it is worth mentioning that for the magnitude of parameter values numerically considered in their paper, the effect of non-Fourier heat transfer is minimal. Furthermore, in the work of Joshi and Majumdar,[10] the "Fourier's law" and "Cattaneo" nonstationary solutions for a simple one-dimensional geometry were directly compared to the analysis from a microscopic Boltzmann treatment; it was comparatively noted that both the Fourier and Cattaneo results were inadequate on short spatial and temporal scales. This comparative analysis points to the notion that microscopic phonon dynamics should be accounted for holistically in order to facilitate a more complete and accurate analysis of the heat redistribution processes in nanodimensional structures. It is worth mentioning that the overwhelming complexity of solving directly the Boltzmann equation, even for relatively simple configurations, brought to existence the advanced simplifying schemes to numerically treat heat redis-

tribution processes, such as the nonlocal heat conduction model,[11] and the ballistic-diffusive heat-conduction equations.[12]

Another intrinsic phonon-mediated loss mechanism is known as the Akhiezer effect.[13] This effect is most commonly considered in relation to the attenuation losses suffered by ultrasonic waves in dielectric crystals at elevated temperatures. In essence, due to anharmonicity, a strain modulates the phonon frequencies (and, most important, differently for different phonon modes); thus, the original phonon distribution becomes distorted and requires a microscopic time to reestablish phonon equilibrium locally. This irreversible process results in an absorption of elastic energy to generate entropy in the phonon subsystem. A simple qualitative treatment of this process was reported by Bömmel and Dransfeld.[14] A more advanced microscopic treatment was developed by Woodruff and Ehrenreich.[15]

Unlike ultrasonic waves in infinite solids, where the scale of the spatial inhomogeneity of the strain pattern is defined solely by the plane-wave frequency through the bulk dispersion law, the strain pattern associated with flexural waves in thin beams and membranes is aptly influenced by the boundary conditions associated with the mechanical motion of the finite material domain. As a result, the spatial and temporal scales of the strain pattern can be controlled more independently. Specifically, sharp spatial inhomogeneity in strain pattern on the relevant scale of the thermal phonon mean free path can be routinely induced by the flexure in the *cross section* of the gigahertz thin beam. This simple observation has direct and important consequences for the magnitude and variation of intrinsic losses in nanoscale resonators.

In the general framework of this paper, the detailed phonon dynamics is established for Euler-Bernoulli flexural beams; as well, phonon-related losses and degradation mechanisms are identified for a mechanical resonator beam configuration as the beam size reduces to the nanodimensional spatial scale and the frequency of operation rises into the low GHz spectral region. The technical approach considers nonequilibrium heat generation and redistribution processes from mechanical strain during high frequency NEMS operation *beyond the conventional heat diffusion and local temperature approximation*. Specifically, a semiclassical phonon dynamical picture is introduced, allowing detailed microscopic analytical and numerical modeling of phonon flow and heat redistribution in Euler-Bernoulli nanoscale resonators. Relevant mechanistic phonon transport regimes and related transition boundaries are identified by delineating the appropriate scaling laws.

In Sec. II, the salient features relevant to the dynamics of the Euler-Bernoulli flexural beams are reviewed and specific attention is devoted to the structure of the spatially inhomogeneous time dependent strain pattern developed inside beam material. Section III is focused on the formulation and analysis of phonon dynamics under the nonequilibrium thermodynamic conditions in flexural nanobeams within a Boltzmann framework; in particular, a reliable quantification of the nanoresonator Q factor is developed in the presence of nondiffusive phonon transport. In Sec. IV, a numerical analysis of the phonon assisted losses in the double clamped flexural NEMS resonator is provided as an illustrative example of the methodology. The functional dependence of the loss on the characteristics of the flexural and phonon systems is established and graphically portrayed. Specifically, domains of phonon-related dissipative mechanisms[7,13] are identified and analyzed in terms of their scaling attributes relative to the key spatial and temporal characteristics of the phonons, i.e., mean free path and phonon relaxation time, as well as the relevant physical parameters of the NEMS structure, i.e., beam thickness, length, and resonator operational frequency. In Sec. V, results are summarized, and further considerations concerning the integrity of Q factor are discussed.

II. PICTURE OF THE BEAM DYNAMICS

Flexural modes available to the double clamped resonator, cantilever (for large *length to thickness* aspect ratios $L/t > 10$), or in the model of an infinite beam (then L is the period of the mode) can be described analytically by the Euler-Bernoulli equation of solid mechanics in the limit of no energy dissipation and in the continuum approximation.[1,16] Applying this long-beam approximation of the Euler-Bernoulli theory, one arrives at the equation for the transverse y displacement $u(z,t)$ for an undriven beam along the direction of its length z as

$$\rho A \frac{\partial^2 u}{\partial t^2} + \frac{\partial^2}{\partial z^2} EI \frac{\partial^2 u}{\partial z^2} = 0.$$

Here, ρ is the material density, A is the area of the beam cross section, E is the Young modulus, I is the cross-sectional area of the moment of inertia (bending moment of inertia), and EI is known as the *flexural rigidity* of the beam. The boundary conditions specify the beam clamping conditions for finite structures. In particular, for the rigidly clamped boundary condition $u=0$ and $u' \equiv \partial u/\partial z = 0$. Thus, for the double clamped resonator (clamped at beam ends at $z=0$ and $z=L$), the eigensolution for a homogeneous beam of a rectangular cross section wt (i.e., $A=wt$ and $I=wt^3/12$), can be written in phasor form as

$$u_n(z,t) = U_n(z) e^{i\Omega_n t},$$

where

$$U_n(z) = C_{n1}[\cos(k_n z) - \cosh(k_n z)] + C_{n2}[\sin(k_n z) - \sinh(k_n z)],$$

with frequency

$$\Omega_n = \sqrt{\frac{EI}{\rho A}} k_n^2 = \sqrt{\frac{E}{\rho}} t k_n^2. \tag{1}$$

Here, k_n is chosen to satisfy the boundary conditions and is a solution of the transcendental equation,

$$\cos(k_n L)\cosh(k_n L) = 1.$$

It is found that $k_n L \approx 4.730$, 7.853, and 10.996 for the first three modes. The fundamental frequency Ω_1 of the oscillator rises as the resonator size and/or aspect ratio (length to thickness) is reduced as desired.

It is noted that while the Euler-Bernoulli theory works well for the relatively long beams, the importance of the

Timoshenko rotational inertia and shear corrections[17] to the beam dynamics increases progressively for smaller L/t ratios. Also, our treatment of double clamped beams here is limited to small flexural vibrations, which assumes that $|U(z)| < t$; nonlinearities are set into play through the quadratic dependence on U in the beam lengthening term,[1] $\Delta L \approx \int_L dz[U'(z)]^2/2$, as larger flexural vibrations affect the resonator dynamics. For particular classes of flexural systems, such as carbon nanotubes with naturally small thicknesses, even very moderate displacements would lead to resonator dynamics beyond the linear regime.[18] On the other hand, for cantilevers, the significance of this deviation from linearity is largely alleviated.

The structure of the strain field corresponding to a particular flexural mode can be established as follows: For thin beams in the linear regime, the situation is very simple,[16] the only nonzero components of the strain tensor are defined by the mode deflection amplitude $u(z)$ as

$$u_{zz} = -y\frac{\partial^2 u}{\partial z^2}, \tag{2}$$

and

$$u_{xx} = u_{yy} = -\sigma u_{zz}, \tag{3}$$

where σ is known as the Poisson ratio. The *trace* of the strain tensor is then,

$$\sum_i u_{ii} = -(1-2\sigma)yu''. \tag{4}$$

The linear energy density along the beam is given in phasor form by

$$h_W(z) = \frac{\rho A\Omega^2}{2}[U(z)]^2 + \frac{EI}{2}[U''(z)]^2,$$

where the first term is the kinetic energy and the second term is the potential energy of flexural deformation of the beam. The kinetic energy density, in phasor form, is proportional to the square of the fundamental mode eigenfunction U_1^2 and the flexural deformation energy is proportional to $[U_1'']$.[2] Both components of the energy distribution are highly peaked along the beam and scale in accordance with L. However, as L is reduced, the *relative* amounts of the kinetic and flexural energies along the beam remain unchanged for the Euler-Bernoulli normalized eigenmode U_1; thus, the kinetic–flexural energy partition could vary with L only by considering the higher order corrections to the Euler-Bernoulli equation.

Finally, the total energy of the mechanical oscillation is given by

$$W = \int_L dz h_W(z). \tag{5}$$

III. PHONONS UNDER NONEQUILIBRIUM THERMODYNAMIC CONDITIONS IN FLEXURAL NANOBEAMS

A quantitative description for the processes of heat generation and redistribution in thin flexural beams is developed by applying the Boltzmann formalism to capture the dynamics of the nonequilibrium phonon distribution resulting from the spatially inhomogeneous mechanical compression and dilation. The appropriate multidimensional integro-differential equation is derived for the phonon distribution function, including the modulation of phonon frequencies by spatially inhomogeneous strain, phonon ballistic transfer, and scattering processes, leading to the thermalization of the phonon ensemble. This treatment allows for a reliable quantification of the phonon flow in the resonator, and an analysis of the quality factor Q in the presence of nondiffusive phonon transport.

A. Phonon Hamiltonian in the presence of strain

The space and time-modulated Hamiltonian for a phonon with the wave vector $\mathbf{q}$ can be written as

$$H = \hbar\omega(\mathbf{q},\mathbf{r},t) = \hbar\omega_0(\mathbf{q})[1+\alpha(\mathbf{q},\mathbf{r},t)];$$

here, for the simplicity of the notation, $\mathbf{q}$ includes both the wave vector and index of the phonon branch. In the presence of strain, the lowest order expression for the modulation coefficient α is given[13] by

$$\alpha(\mathbf{q},\mathbf{r},t) = -\sum_{ik}\gamma_{ik}(\mathbf{q})u_{ik}(\mathbf{r},t), \tag{6}$$

where u_{ik} is the strain tensor and $\gamma_{ik}(\mathbf{q})$ is the *generalized Grüneisen tensor*.[15] The only nonzero components of the strain tensor in the beam are those in Eqs. (2) and (3) above. Then, one can write explicitly from Eq. (6),

$$\alpha(\mathbf{q},y,z,t) = \left[(1+\sigma)\gamma_{zz}(\mathbf{q}) - \sigma\sum_i \gamma_{ii}(\mathbf{q})\right]yu''(z,t). \tag{7}$$

In replacing all of the diagonal tensor components γ_{ii} with a *single* Grüneisen constant γ, we can reduce Eq. (7) further, so that,

$$\alpha = -\gamma\sum_i u_{ii} = (1-2\sigma)\gamma yu''(z,t). \tag{8}$$

The simplification that γ assumes a scalar and q-independent form was invoked historically in the early development of the bulk thermal expansion theory and has served well in simple situations requiring only the averages over the bulk phonon spectrum; however, in the limiting case of a nanoregime, the averaging with respect to $\Sigma_i\gamma_{ii}$ and γ_{zz} is not easily justified, especially when one needs to accommodate the inherent physically present spatial anisotropy of the system in the analysis of the degradation processes. Moreover, it follows that in choosing $\gamma_{ij}(\mathbf{q})$ as a single constant, it *artificially precludes* the manifestation of the Akhiezer effect; in order to preserve the physical presence of the Akhiezer phenomena, potentially important at the NEMS spatial and frequency scale yet keep the analysis tractable, one could allow for two different constants γ_1 and γ_2 to mimic the variation in tensor $\gamma_{ij}(\mathbf{q})$—an approach originally proposed by Bömmel and Dransfeld.[14] This two parameter approach is utilized later in this section.

B. Boltzmann equation

The quantitative description of the heat generation and redistribution processes in thin flexural beams is developed using the Boltzmann formalism. The linearized Boltzmann equation is derived to capture the responsive development of the nonequilibrium phonon distribution resulting from the spatially inhomogeneous mechanical compression and dilation during flexure. For the instantaneous distribution function $N(\mathbf{q},\mathbf{r},t)$ for the population of the phonons in the beam, the Boltzmann equation is expressed as

$$\left(\frac{\partial N}{\partial t}\right)_{\text{coll}} = \frac{\partial N}{\partial t} + \frac{\partial N}{\partial \mathbf{r}} \cdot \frac{\partial \omega}{\partial \mathbf{q}} - \frac{\partial N}{\partial \mathbf{q}} \cdot \frac{\partial \omega}{\partial \mathbf{r}}.$$

Splitting N into the "equilibrium" part $N_0(\hbar\omega/kT_0)$, corresponding to the local phonon frequencies ω defined by the spatially inhomogeneous strain and the *true equilibrium* temperature T_0, and the nonequilibrium part,

$$N_1(\mathbf{q},\mathbf{r},t) = N(\mathbf{q},\mathbf{r},t) - N_0(\hbar\omega/kT_0), \tag{9}$$

one can linearize the original Boltzmann equation for the phonon distribution function to arrive at[19]

$$\left(\frac{\partial N}{\partial t}\right)_{\text{coll}} = \frac{\partial N_1}{\partial t} + N_0' \frac{\hbar\omega_0}{kT_0}\frac{\partial \alpha}{\partial t} + \mathbf{v}_0 \cdot \frac{\partial N_1}{\partial \mathbf{r}}. \tag{10}$$

Here,

$$N_0(\omega,T) \equiv N_0(\hbar\omega/kT) = [\exp(\hbar\omega/kT) - 1]^{-1}$$

is the thermal equilibrium distribution function, N_0' is its derivative in respect to $x=\hbar\omega/kT$, and $\mathbf{v}_0=\partial\omega_0/\partial\mathbf{q}$ is the mode velocity.

Invoking the effective relaxation time approximation, one can write for the collisional term,

$$\left(\frac{\partial N}{\partial t}\right)_{\text{coll}} = \frac{N - N_0(\omega,T)}{\tau_{\text{ph}}}, \tag{11}$$

where $\tau_{\text{ph}}(\mathbf{q})$ is the phonon relaxation time. There are a number of subtle issues associated with Eq. (11). First, it is a heuristic approximation to the realistic microscopic description for the phonon-phonon interactions.[20] Even then, actually two classes of phonon-phonon scattering processes take place: The *normal* processes that conserve total momentum of the colliding pair and umklapp processes that do not conserve total momentum. As written in Eq. (11), it is implicitly assumed that the umklapp processes dominate so that the asymptotic phonon distribution can be characterized by a single parameter—local equilibrium temperature T. Furthermore, this local equilibrium temperature T should not be defined by averaging the phonon distribution only at a single spatial point; instead, it should be obtained by averaging over the area of the size of about l_{ph}. Thus, it is clear that T should approach T_0 as the beam thickness becomes smaller than l_{ph}. Nevertheless, it was shown[15] that treating T as a single-point quantity should produce comparable results for the losses even in the limit of $t<l_{\text{ph}}$.

Now, we consider a case of substantially different spatial scales $L \gg t$, suitable for the Euler-Bernoulli-Boltzmann resonator. In particular, this allows for the treatment of all thermal transfer as essentially *one-dimensional*—taking place along the y axis in the plane of the beam cross section. Linearizing the collision term of Eq. (11) with help of Eq. (9), and then seeking oscillatory solutions of Eq. (10) for N_1 with flexural fundamental frequency Ω, we obtain for N_1,

$$(1 - i\Omega\tau_{\text{ph}})N_1 - v_0\tau_{\text{ph}}\cos\theta N_1' = N_0'\frac{\hbar\omega_0}{kT_0}\left(i\Omega\tau_{\text{ph}}\alpha - \frac{T_1}{T_0}\right). \tag{12}$$

Here, the spatial variation of α is given by Eq. (8) and the temperature difference $T_1=T-T_0$ is defined by the total energy balance in the scattering processes, i.e.,

$$\frac{1}{8\pi^3}\int d\mathbf{q}\hbar\omega\left(\frac{\partial N}{\partial t}\right)_{\text{coll}} = 0. \tag{13}$$

Further analytical progress can be made by making several simplifying assumptions: (i) assume the Debye model $\omega_0(\mathbf{q})=c_0q$ with the q-independent velocity $v_0\equiv c_0$ for the phonon spectrum; and (ii) assume that the relaxation time τ_{ph} is also phonon mode-independent. Then, in treating the collisional term in the relaxation approximation and expanding Eq. (13) for the energy balance to first order, one obtains,

$$\frac{1}{4\pi^2}\int d\cos\theta\int dqq^2\hbar\omega(q)N_1 = -\frac{T_1}{2\pi^2}\int dqq^2\left[\frac{\hbar\omega_0(q)}{kT_0}\right]^2 kN_0'. \tag{14}$$

The equation for the right hand side (rhs) is easily recognized; the specific heat of phonon mode q is

$$S(q) = -\left[\frac{\hbar\omega_0(q)}{kT_0}\right]^2 kN_0',$$

and the heat capacity of the phonon subsystem (per unit volume) is

$$C = \frac{1}{2\pi^2}\int dqq^2 S(q);$$

therefore, the rhs of Eq. (14) reduces to CT_1.

Furthermore, assuming the Grüneisen tensor γ to be a q-independent scalar constant as given by Eq. (8), one can multiply Eq. (12) by a phonon energy and then integrate over modulus q to get an equation for the partially integrated phonon distribution function,

$$f(y,\cos\theta,z) \equiv \frac{1}{2\pi^2}\int dqq^2\hbar\omega_0 N_1.$$

Explicitly, one gets,

$$(1 - i\Omega\tau_{\text{ph}})f - l_{\text{ph}}\cos\theta f_y' = C[T_1 - i\Omega\tau_{\text{ph}}T_0\alpha(y,z)], \tag{15}$$

with Eq. (14) reducing to,

$$\frac{1}{2}\int_{-1}^{1} d\cos\theta f = CT_1.$$

Using Eq. (8) to express $\alpha(y,z)$ via γ and the flexural mode deflection $U(z)$, it is convenient to further introduce a function $\tilde{f}(\tilde{y},\cos\theta)$ as

$$f(y,\cos\theta,z) \equiv CT_0(1-2\sigma)tU''(z)\tilde{f}(\tilde{y},\cos\theta),$$

where $\tilde{y}=y/t$. Here, the advantage lies in the explicit factorization of the z dependence, i.e., $\tilde{f}$ is functionally the same along the beam length and satisfies the equation,

$$(1-i\Omega\tau_{\rm ph})\tilde{f} - \tilde{l}_{\rm ph}\cos\theta\tilde{f}_{\tilde{y}} = \tilde{F} - i\Omega\tau_{\rm ph}\gamma\tilde{y}, \tag{16}$$

where $\tilde{l}_{\rm ph}=l_{\rm ph}/t$ is a dimensionless system parameter and $2\tilde{F}(\tilde{y}) \equiv \int d\cos\theta\tilde{f}$. Note that, alternatively, one could decide to introduce $\tilde{y}=y/l_{\rm ph}$, $\tilde{t}=t/l_{\rm ph}$, and $\tilde{l}_{\rm ph}\equiv 1$, but our choice seems to result in a slightly more transparent scaling law analysis for loss in the resonator. Lastly, Eq. (16) needs to be accompanied by physically appropriate boundary conditions[21] and then solved either numerically directly or as a series expansion.

In addressing the boundary condition, it is instructive to present f as a sum of two functions: one symmetric with respect to the angular argument of $\cos\theta$ and the other antisymmetric with respect to $\cos\theta$; therefore,

$$\tilde{f} = \tilde{f}_s + \tilde{f}_a.$$

Then $2\tilde{F} \equiv \int d\cos\theta\tilde{f} = \int d\cos\theta\tilde{f}_s$ alone, whereas $\tilde{f}_a$ can be expressed via $\tilde{f}_s$ with an equation for $\tilde{f}_s$ given by,

$$(1-i\Omega\tau_{\rm ph})^2\tilde{f}_s - \tilde{l}_{\rm ph}^2\cos^2\theta\tilde{f}_s'' = (1-i\Omega\tau_{\rm ph})[\tilde{F} - i\Omega\tau_{\rm ph}\gamma\tilde{y}].$$

Thus, in the case of perfectly reflecting boundary conditions,[21] function $\tilde{f}_a$ vanishes at the beam edges, which corresponds to $\tilde{f}_s'=0$ at $\tilde{y}=\pm 1/2$. Expressing the solution for f_s as an expansion,

$$\tilde{f}_s(\tilde{y},\theta) = \sum_m \tilde{f}_{s,m}(\theta)\sin(2m+1)\pi\tilde{y}, \tag{17}$$

and noticing that, identically,

$$\tilde{y} = \sum_m \tilde{y}_m \sin(2m+1)\pi\tilde{y},$$

with coefficients $\tilde{y}_m \equiv 2(-1)^m/\pi^2(2m+1)^2$, it follows that the coefficients $\tilde{f}_{s,m}$ and their related angular integrals $\tilde{F}_m$ can then be calculated *analytically* without much difficulty.

C. Phonon related losses in flexural beams—a single constant scalar Grüneisen coefficient

As already mentioned in previous discussion, the problem of losses in flexural beams is conceptually similar to a problem of sound attenuation in bulk dielectric crystals.[14,15] In the *bulk* discussions, an infinite domain with solutions in the form of plane waves was analyzed; in this paper, the finite boundaries force solutions on the finite domain in the presence of spatial inhomogeneities. The energy conservation law enforces the condition that the average rate at which the energy is removed from the flexural vibration is equal, in the steady state process, to the rate of transferring energy from the phonon system to the heat bath[22] through

$$Z = -\sum_{q,j}\left\langle H\left(\frac{\partial N}{\partial t}\right)_{\rm coll}\right\rangle. \tag{18}$$

Using Eq. (10) to express the collisional term in Eq. (18) via the time derivative of N and drift and diffusion terms, and further removing terms that time average to zero in the steady process, it is found that,

$$Z = \frac{1}{16\pi^3}\int_V d\mathbf{r}\int d\mathbf{q}\hbar\omega_0\,{\rm Re}\left\{N_1^*\frac{\partial\alpha}{\partial t}\right\}. \tag{19}$$

With inverse resonator quality factor Q formally defined as the fraction of the oscillation energy lost per radian of flexural vibration, i.e.,

$$Q^{-1} = \frac{Z}{\Omega W}, \tag{20}$$

the final result for quality factor is found after substituting the expression for the total flexural energy W given by Eq. (5) and the average rate of energy transfer Z defined by Eq. (19) into Eq. (20).

In utilizing the previously made approximations: (i) a large beam aspect ratio, (ii) the Debye model, and (iii) a single constant scalar Grüneisen coefficient, one can perform a number of partial integrations to reduce Eq. (19) to

$$Z = \Omega\frac{(1-2\sigma)^2CT_0\gamma wt^3}{2}\int_L dz[U''(z)]^2\int d\tilde{y}\tilde{y}\,{\rm Im}\{\tilde{F}(\tilde{y})\}, \tag{21}$$

in terms of function $\tilde{F}$ for a beam mode U. This gives

$$Q^{-1} = 6(1-2\sigma)^2CT_0E^{-1}\gamma\int d\tilde{y}\tilde{y}\,{\rm Im}\{\tilde{F}(\tilde{y})\}. \tag{22}$$

With N_1 (or $\tilde{f}$ and its $\cos\theta$-integral $\tilde{F}$) determined, phonon-related losses in the beam can be numerically evaluated. In particular, if $\tilde{f}$ is expressed as a series expansion of the form given in Eq. (17), then,

$$Q^{-1} = 6(1-2\sigma)^2CT_0E^{-1}\gamma\sum_m \tilde{y}_m\,{\rm Im}\{\tilde{F}_m\}. \tag{23}$$

Here, it is stressed that when the assumption of one-dimensional thermal transport (case of a relatively long beam, that is $L \gg t$) is not valid, N_1 cannot be factorized to effectively separate the coordinate z along the beam, thus, leaving us with a more complex system of partial differential equations to be solved numerically.

D. Losses in the presence of the Akhiezer effect

Adapting a heuristic based on only a single Grüneisen constant precludes the manifestation of the Akhiezer effect.

Therefore, a heuristic which allows us to capture the Akhiezer effect is now developed. As a starting point in considering losses in acoustic waves in solids, Bömmel and Darnsfeld[14] have split all phonon modes into two distinguished groups—those experiencing positive temperature changes and those experiencing negative or no temperature changes. Following Ref. 14, we too assumed that all phonon states can be split into two global groups labeled "1" and "2," with portion p_1 of all phonons belonging to the first group and portion $p_2=1-p_1$ belonging to the second one. Both groups are further assumed to have an exactly identical spectrum in absence of strain. For simplicity, the effect of the applied strain will be controlled by mode-independent (for each of two groups) Grüneisen constants γ_1 and γ_2. Then (the symmetric portions of) the phonon distribution functions f_{is} in each group ($i=1,2$) can be found as a solution to the system of equations,

$$(1-i\Omega\tau_{\rm ph})^2\tilde{f}_{is}-\tilde{l}_{\rm ph}^2\cos^2\theta\tilde{f}_{is}''=(1-i\Omega\tau_{\rm ph})[\tilde{F}-i\Omega\tau_{\rm ph}\gamma_i\tilde{y}],$$

with $\cos\theta$-integrals defined as

$$2\tilde{F}_i\equiv\int d\cos\theta\tilde{f}_{is},\quad \text{and}\quad \tilde{F}=p_1\tilde{F}_1+p_2\tilde{F}_2.$$

Solving this system analytically via series expansion, allows to obtain Q as

$$Q^{-1}=6(1-2\sigma)^2CT_0E^{-1}\sum_m\tilde{y}_m\,\mathrm{Im}\{p_1\gamma_1\tilde{F}_{1,m}+p_2\gamma_2\tilde{F}_{2,m}\}. \tag{24}$$

IV. NUMERICAL ANALYSIS AND DISCUSSION

In Fig. 1, graphical analysis for the phonon-related losses (Q^{-1}) is presented in frequency–beam thickness (Ω,t) coordinates (logarithmic scales) for the double clamped flexural resonator. The magnitude of the loss is indicated by the color code: light for high Q or low losses; dark for low Q or high losses. The thickness and the frequency axes to the left and bottom of the graph are scaled in dimensionless units, $t/l_{\rm ph}$ and $\Omega\tau_{\rm ph}$, respectively. Corresponding values for the right and top axes are scaled specifically for crystalline silicon (Si) at room temperature. Taking for Si the standard values of the sound velocity $c=5.86$ km/s, the thermal conductivity $\kappa=160$ W/mK, and the heat capacity (per unit volume) $C=1.64\times10^6$ J/m^3 K, one obtains for the characteristic *phonon* microscopic time constant $\tau_{\rm ph}\approx10$ ps, which corresponds to the phonon mean free path $l_{\rm ph}=c\tau_{\rm ph}\approx50$ nm. Other Si-specific numbers used in the present analysis are as follows:[6] density $\rho=2330$ kg/m^3, Young's modulus $E=1.69\times10^{11}$ kg/m s^2, and the (linear) thermal expansion coefficient $\alpha_T=2.8\times10^{-6}$ K^{-1}. These define the value of the average Grüneisen constant $\overline{\gamma}$ as ≈0.29. Also, the Poisson ratio $\sigma=0.27$ is used.

In these graphs, the position of beams with length-to-thickness aspect ratios of $L/t=5$, and 10 is marked by dotted lines as indicated. As appropriate to the Euler-Bernoulli approximation, the analysis of the thermal phonon flow is conducted for the case $L\gg t$ as well as $L\gg l_{\rm ph}$; in this case, the simplifying assumption is invoked that phonon heat transfer is primarily one-dimensional. Thus, only beam sizes with $L\gtrsim5t$ (and with t not too much less than $t=l_{\rm ph}$) are treated rigorously (lower left part of the graphs). Serious deviation can be expected when these assumptions are not satisfied.

The Q values in Fig. 1 are calculated from Eq. (24), which is generally parametrized to reflect losses in the presence of the Akhiezer effect. Specifically, three distinguishable cases are considered in the framework of the generalized Bömmel–Dransfeld approach: (a) $\gamma_1=\gamma_2\equiv\overline{\gamma}$, (b) $\gamma_1\equiv\overline{\gamma}=-\gamma_2$, and (c) $\gamma_1\equiv2\overline{\gamma}\neq0$, $\gamma_2=0$. For all cases, we have chosen the proportions of the two groups of phonons to be $p_1=p_2=0.5$.

On physical grounds, results reflected in these graphs can be conveniently analyzed with the help of the well-known Zener model.[5] As a background discussion relevant to this model, macroscopic relations, such as the linear stress-strain relation, with Young modulus E serving as a coefficient of proportionality often deemphasize, for simplicity, the aspect of temporal evolution. More generally, E is a function of the modulation frequency Ω and is neither necessarily constant, nor necessarily real, thus, giving rise to loss and memory effects. The reason for this temporal aspect is that there is a finite time necessary for the statistical correlations in the bath to adjust to the system motion; therefore, friction (internal friction) arises as a result of the nonlinear interaction of the system with the bath, leading to transfer of excess potential and kinetic energy from system to the bath. The magnitude of friction is typically proportional to the ensemble average of the system velocity (e.g., du/dt).

A simple (and popular) phenomenological generalization of the static Hooke's law allowing build up time for strain and stress[4] leads to Lorentzian peaks in both the imaginary part of Young's modulus $E(\Omega)$ and loss factor Q^{-1}. This generalization, which is the basis of Zener's model, suggests that in the presence of the relaxation processes with characteristic time τ, the inverse quality factor (losses) as a function of the oscillation frequency Ω can be described by a universal dependence,

$$Q^{-1}=\Delta\frac{\Omega\tau}{1+\Omega^2\tau^2}.$$

It is clear that this functional dependence has a peak at $\Omega_{\rm peak}=\tau^{-1}$. On a log–log scale, this peak manifests itself as a distinctive symmetric hump with 45° slopes: for $\Omega\tau\ll1$, the processes are "isothermal" with a high level of environmental adjustment achieved during operation while in the opposite limit of $\Omega\tau\gg1$, the motion is adiabatic as any adjustment in the bath is too slow to result in notable friction. In the presence of several relaxation mechanisms, several peaks of different magnitudes (defined by the value of Δ) will be observed.

For the fixed beam thickness, case (a) demonstrates a well defined single peak in the losses as a function of frequency. On the log–log (Ω,t) map, peak position follows a piecewise linear dependence with a crossover region corresponding approximately to $t=l_{\rm ph}$. At large beam thicknesses, the slope of the linear dependence corresponds to $t_{\rm peak}\propto\Omega_{\rm peak}^{-1/2}$ while at

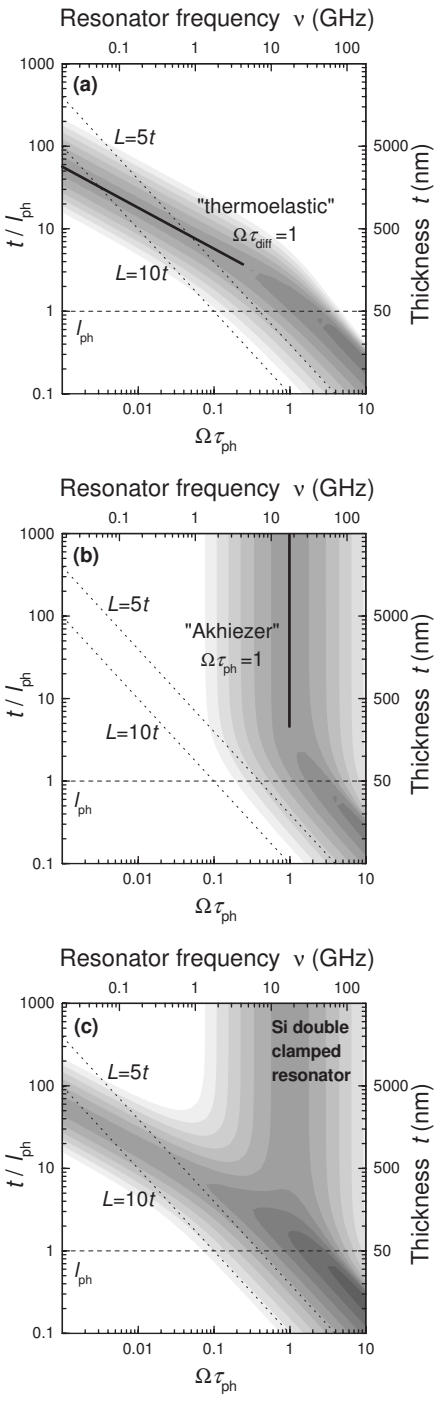

FIG. 1. Magnitude of phonon assisted losses in Si double clamped resonator at room temperature as a function of the flexural frequency Ω and the beam thickness t. Color code: light—high Q, low losses; dark—low Q, high losses. (a) single Grüneisen constant—pure case of thermoelastic losses. At $t \approx l_{ph}$, the character of phonon transport changes from diffusive to ballistic (Fourier vs non-Fourier heat transfer). (b) Two exactly equivalent groups of phonon states with opposite Grüneisen constants—losses dominated by the Akhiezer effect. (c) Interplay of both mechanisms (here, we assume equality of the thermoelastic and microscopic phonon-phonon prefactors). Strictly speaking, only the lower left part of the maps with $L \gtrsim 5t$ satisfies the assumptions of the Euler-Bernoulli theory; furthermore, the assumption of essentially one-dimensional phonon transport requires $L \gg l_{ph}$.

small thicknesses, the slope is $t_{peak} \propto \Omega_{peak}^{-1}$. As the Zener model suggests, the position of this peak can be identified with a characteristic time $\tau = \Omega_{peak}^{-1}$, defining some relaxation process. From the slope of the peak position dependence, one can further deduce scaling of τ with t. At large thicknesses, this characteristic time scales as t squared, which is typical for diffusive processes. Indeed, since case (a) presents a scenario of a single Grüneisen constant, frequencies of all phonons are proportionally modified by strain and no disturbances in the local phonon distribution are created, although, as a whole, the phonon distribution function corresponds to a different temperature, i.e., the phonon population is either heated or cooled. Thus, the only relevant process is the dynamical spatial redistribution of phonons. At large beam thicknesses, this spatial redistribution is dominated by diffusive transport (defining Fourier heat transfer) and is temporally slow with $\tau_{diff} \propto t^2$. That is the microscopic phonon picture representation of the classical thermoelastic loss mechanism originally considered by Zener. As the beam thickness is reduced to become comparable to the phonon mean free path, the scaling of the peak position changes noticeably to $\tau \propto t$ to reflect a transition to ballistic phonon transfer across the beam giving rise to the non-Fourier heat flow, typical at short times and distances.

Case (b) provides conditions for a clear observation of the Akhiezer effect. Since average $\overline{\gamma} = p_1\gamma_1 + p_2\gamma_2 = 0$, the local phonon temperature is not changed and the macroscopic heat transfer does not take place. On the other hand, the local phonon distribution is disturbed. Thus, the main process is the *spatially local* intergroup (interbranch) thermal relaxation, which is, obviously, defined by the microscopic characteristic time τ_{ph}. As a result, the peak position closely corresponds to $\Omega_{peak}\tau_{ph} = 1$ and shows no dependence on beam thickness for a substantially thick resonator. As the sharp spatial inhomogeneities are introduced at $t \approx l_{ph}$, the phonon ballistic transfer process becomes, first, comparable in efficiency to interbranch relaxation and, later, dominates—the regime changes and the peak position acquires dependence on the mode frequency.

Case (c) with $\gamma_1 \equiv 2\overline{\gamma} \neq 0$, $\gamma_2 = 0$ demonstrates the realization of a system where both thermoelastic and Akhiezer's mechanisms are present and of comparable strengths. As the beam parameters vary, their interplay results in a complex behavior of loss factor, captured in Fig. 1(c). In particular, two peaks are present at large beam thicknesses, which merge and change their character as ballistic transfer becomes dominant.

For a given material, the pair of parameters γ_1 and γ_2 can be uniquely specified. This can be realized through careful evaluation of the average values and variations in the mode specific Grüneisen constants available through experimentally tabulated data for different phonon branches or through values calculated from the second and third order elastic moduli.[15,21] It follows from provided data that the constants γ_1 and γ_2 are typically highly unequal in magnitude, with say $|\gamma_1| \gg |\gamma_2|$, favoring the choice made in case (c). It should be noted that our approach can be easily generalized to incorporate more than two groups of phonons, although we feel that this further increase in complexity is unlikely to capture any substantially new phenomena.

To put our numbers into perspective, the variation of Q^{-1} over the range of one and a half decades from its maximum is explicitly displayed in Fig. 1. For the material parameters chosen, the peak values of loss in both the thermoelastic (diffusive) and Akhiezer regimes correspond to $Q \approx 7.5 \times 10^4$ while in the ballistic regime, with absolute maximum in the lower right corner, the peak loss has a Q value of $\approx 2.2 \times 10^4$.

Overall, the following quantitative observations can be made:

(i) Thermoelastic mechanism dominates in thick beams with large aspect ratio well described by Euler-Bernoulli beams. In particular, with scaling down Si beam, the peak in losses is achieved at subgigahertz frequencies, after that, the quality factor improves.

(ii) At about $t = l_{\mathrm{ph}}$, the character of the phonon transfer changes to ballistic, leading to a different scaling of the peak position on the (Ω, t) map; this leads to saturation of losses with further reduction of the structure.

(iii) Akhiezer effect is of minor importance for structures with large aspect ratio well described by Euler-Bernoulli equation. It noticeably contributes to losses only at the onset of the regime of the ballistic phonon transfer where both mechanisms merge.

(iv) In quantitative terms, at 1–10 GHz frequencies, a Si NEMS resonator with $L = 5t$ has substantially higher losses than a $L = 10t$ resonator.

V. SUMMARY AND CONCLUSIONS

In summary, during gigahertz frequency operation, the phonon subsystem inside a flexural NEMS beam evolves into a unique nonequilibrium dynamics due to a highly inhomogeneous strain pattern. Resulting nonequilibrium heat generation and redistribution processes have been treated beyond the conventional heat diffusion and local temperature approximation. An advanced theoretical analysis was formulated and conducted in the Boltzmann framework to capture the appropriate phonon dynamics inside flexural beams. In the resulting study, the intrinsic mechanisms and related analytic principles, including scaling rules influencing NEMS degradation, have been developed and expressed in a user-friendly form for application.

The intriguing question of prohibitive high-Q operation based on fundamental physical limitations and degradation was also raised in this study. Overall, our analysis, using a limited parameter set, shows no degradation in quality factor with progressive miniaturization from thermoelastic and Akhiezer effects; however, there appears to be a marginal softening in quality factor observed for the Akhiezer component when $\Omega \tau_{\mathrm{ph}} > 1$ as noted in Fig. 1. Yet, it is commonly reported in numerical and experimental NEMS studies that reduction in resonator length leads to substantial reduction in the quality factor Q.[23,24] These observations tentatively suggest that with down scaling, the microresonator losses are determined, to a large extent, by surface related processes; in fact, a larger fraction of the beam atoms reside at the surface, so that the surface-to-volume (S/V) component grows linearly with beam miniaturization. Therefore, it is likely that an alternative mechanism such as enhancement of the third and fourth-order anharmonic phonon-phonon interactions in the presence of the static strain in the surface layer might lead to the direct dependence on the phonon characteristic time $\tau_{\mathrm{ph}}^{\mathrm{beam}}$ on the surface-to-volume ratio. Such an anharmonic effect can be incorporated into the general description of the phonon flow of this analysis through a set of heuristic parameters describing scattering and thermalization due to surfaces or interfaces. This will be the natural extension of the present investigation.

ACKNOWLEDGMENTS

This research was supported in part by the (U.S.) Army Research Office and the National Science Foundation.

*Previously at the Department of Electrical and Computer Engineering, North Carolina State University.

[1] A. N. Cleland, *Foundations of Nanomechanics* (Springer-Verlag, Berlin, 2003).
[2] J. A. Pelesko and D. H. Bernstein, *Modeling MEMS and NEMS* (CRC, Boca Raton, FL, 2002).
[3] A. S. Novick and B. S. Berry, *Anelasic Relaxation in Crystalline Solids* (Academic, New York, 1972).
[4] W. Voigt, *Lehrbuch der Kristallphysik* (Teubner, Leipzig, 1928); A. Ballato, IEEE Trans. Sonics Ultrason. **SU-25**, 107 (1978).
[5] C. Zener, Phys. Rev. **52**, 230 (1937); **53**, 90 (1938).
[6] A. N. Cleland and M. L. Roukes, J. Appl. Phys. **92**, 2758 (2002).
[7] R. Lifshitz and M. L. Roukes, Phys. Rev. B **61**, 5600 (2000).
[8] F. L. Guo and G. A. Rogerson, Mech. Res. Commun. **30**, 513 (2003).
[9] Y. Sun, D. Fang, and A. K. Soh, Int. J. Solids Struct. **43**, 3213 (2006).
[10] A. A. Joshi and A. Majumdar, J. Appl. Phys. **74**, 31 (1993).
[11] G. D. Mahan and F. Claro, Phys. Rev. B **38**, 1963 (1988).
[12] G. Chen, Phys. Rev. Lett. **86**, 2297 (2001).
[13] A. Akhiezer, J. Phys. (USSR) **1**, 277 (1939).
[14] H. E. Bömmel and K. Dransfeld, Phys. Rev. **117**, 1245 (1960).
[15] T. O. Woodruff and H. Ehrenreich, Phys. Rev. **123**, 1553 (1961).
[16] L. D. Landau and E. M. Lifshitz, *Theory of Elasticity* (Pergamon, Oxford, 1959).
[17] S. P. Timoshenko and J. N. Goodier, *Theory of Elasticity* (McGraw-Hill, New York, 1970).
[18] C. H. Ke, H. D. Espinosa, and N. Pugno, J. Appl. Mech. **72**, 726 (2005); N. Pugno, C. H. Ke, and H. Espinosa, *ibid.* **72**, 445 (2005).
[19] It is worth noting that this particular linearization is different from another commonly performed splitting , where frequency ω_0 is used instead of ω in the *true*, i.e., unstrained, equilibrium part — an approach used, for example, in Ref. 15.

[20] P. G. Klemens, in *Lattice Dynamics IIIB*, edited by W. P. Mason (Academic, New York, 1965), p. 201.
[21] J. M. Ziman, *Electrons and Phonons: The Theory of Transport Phenomena in Solids* (Oxford University Press, Oxford, 2001).
[22] E. I. Blount, Phys. Rev. **114**, 418 (1959).
[23] R. E. Mihailovich and N. C. MacDonald, Sens. Actuators, A **50**, 199 (1995).
[24] R. E. Rudd and J. Q. Broughton, J. Mod. Sim. Microsys. **1**, 29 (1999); J. Q. Broughton, C. A. Meli, P. Vashishta, and R. K. Kalia, Phys. Rev. B **56**, 611 (1997).